



UvA-DARE (Digital Academic Repository)

Electronic state of pristine and intercalated Sc₃N@C₈₀ metallofullerene

Alvarez, L.; Pichler, T.; Georgi, P.; Schwieger, T.; Peisert, H.; Dunsch, L.; Hu, Z.; Knupfer, M.; Fink, J.; Golden, M.S.; Bressler, P.; Mast, M.

Published in:
Physical Review B

[Link to publication](#)

Citation for published version (APA):

Alvarez, L., Pichler, T., Georgi, P., Schwieger, T., Peisert, H., Dunsch, L., ... Mast, M. (2002). Electronic state of pristine and intercalated Sc₃N@C₈₀ metallofullerene. *Physical Review B*, 66, 035107.

General rights

It is not permitted to download or to forward/distribute the text or part of it without the consent of the author(s) and/or copyright holder(s), other than for strictly personal, individual use, unless the work is under an open content license (like Creative Commons).

Disclaimer/Complaints regulations

If you believe that digital publication of certain material infringes any of your rights or (privacy) interests, please let the Library know, stating your reasons. In case of a legitimate complaint, the Library will make the material inaccessible and/or remove it from the website. Please Ask the Library: <http://uba.uva.nl/en/contact>, or a letter to: Library of the University of Amsterdam, Secretariat, Singel 425, 1012 WP Amsterdam, The Netherlands. You will be contacted as soon as possible.

Electronic structure of pristine and intercalated $\text{Sc}_3\text{N}@C_{80}$ metallofullereneL. Alvarez,¹ T. Pichler,^{1,2} P. Georgi,¹ T. Schwieger,¹ H. Peisert,¹ L. Dunsch,¹ Z. Hu,¹ M. Knupfer,¹ J. Fink,¹ P. Bressler,³ M. Mast,³ and M. S. Golden⁴¹*Institute of Solid State Research, IFW Dresden, P.O. Box 270016, D-01171 Dresden, Germany*²*Institute of Materials Physics, University of Vienna, Strudlhofgasse 4, 1090 Vienna, Austria*³*BESSY GmbH, Albert Einstein Strasse 15, 12489 Berlin, Germany*⁴*Van der Waals-Zeeman Institute for Experimental Physics, Universiteit van Amsterdam, NL-1018 XE Amsterdam, The Netherlands*

(Received 30 January 2002; published 9 July 2002)

We report a study of the electronic structure and charge transfer in the metallofullerene $\text{Sc}_3\text{N}@C_{80}$ using photoemission and x-ray absorption spectroscopy. Through a comparison of the x-ray absorption spectrum of $\text{Sc}_3\text{N}@C_{80}$ at the Sc $L_{2,3}$ edge with atomic multiplet calculations, the Sc $3d$ electron count is determined to be 0.6, thus giving an effective Sc valency of 2.4. With the N atom gaining a full electronic shell by means of covalent bonding with the Sc (also involving the Sc $3d$ electron density observed in the x-ray absorption experiments), the remaining six valence electrons of the Sc_3N cluster are then transferred to the carbon cage which stabilizes the C_{80} cage structure with I_h symmetry, a structure which is not energetically favored in neutral C_{80} . The presence of the highly symmetric I_h cage structure is further supported by the observation of distinct fine structure in the valence band photoemission spectra of the endohedral, which results from the high degree of effective degeneracy of the electronic states in the molecule. Finally, the results of investigations of K-doped $\text{Sc}_3\text{N}@C_{80}$ using photoemission give insight into the $\text{K}_x\text{Sc}_3\text{N}@C_{80}$ phases that are formed upon intercalation.

DOI: 10.1103/PhysRevB.66.035107

PACS number(s): 73.61.Wp, 71.20.Tx, 79.60.-i, 78.70.Dm

I. INTRODUCTION

After the extensive studies in the past several years of novel carbon nanostructures such as fullerenes or carbon nanotubes, many fundamental investigations are now carried out on the electronic properties of endohedral compounds. Particularly, charge transfer in metallofullerenes where the fullerene molecule can encage different species such as La, Y, Tm, Gd, or Sc has been widely investigated,¹⁻⁷ as these materials are expected to display remarkable electronic and structural properties associated with this charge transfer from the metal to the carbon cage. More recently, the encapsulation of fullerene molecules into nanotubes, giving so-called peapods,⁸ and even the encapsulation of metallofullerenes into single wall nanotubes⁹ has been reported and should extend this interest since these novel materials might display extremely interesting electronic properties. Generally, for the metallofullerenes, an ionic interaction between the endohedral molecule and the carbon cage is to be seen as a crude picture and hybridization effects have to be taken into account.^{1,5,6,9}

Recently, the discovery was made that the introduction of a small amount of nitrogen into the metallofullerene reactor favors the formation of a new family of stable endohedral fullerenes $\text{A}_x\text{B}_{3-x}\text{N}@C_{80}$ ($x=0-3$).^{10,11} One prominent member of this new family is $\text{Sc}_3\text{N}@C_{80}$. The nuclear magnetic resonance (NMR) spectrum of $\text{Sc}_3\text{N}@C_{80}$ has only two lines, consistent with I_h symmetry for the fullerene cage.¹⁰ It is well known that the symmetry of stable pristine C_{80} is D_2 (Ref. 12) and this is supported by calculations.^{2,3,7,13-15} These calculations also discuss the stability of the seven C_{80} isomers allowed by the isolated pentagon rule, as a function of a charge transfer to the fullerene cage. On going from the neutral to a C_{80}^{4-} state, the icosahedral C_{80} is predicted to

switch from being the least stable to the most stable carbon cage.¹³ This I_h structure could become even more energetically favorable in the C_{80}^{6-} state.^{2,3,7,13-15} Therefore it seems natural to suggest that the C_{80} cage with I_h symmetry is stabilized by charge transfer from the nitride cluster in $\text{Sc}_3\text{N}@C_{80}$. The exact amount of charge transfer, however, has up to now been unknown and should be determined experimentally, not only to settle this specific question, but also to further our knowledge of these novel encapsulated transition metal nitride fullerene clusters in general.

In this study, we report results regarding the charge transfer and the electronic structure of pristine and potassium intercalated $\text{Sc}_3\text{N}@C_{80}$. X-ray absorption experiments at the Sc $L_{2,3}$ edge are compared to atomic multiplet calculations including charge transfer in order to derive the effective valency of Sc. This method is well established in the experimental determination of the valency of transition metal compounds^{16,17} and has also been recently applied to metallofullerenes where the mainly trivalent character of the Sc ions could be proven in $\text{Sc}_2@C_{84}$.⁵ For $\text{Sc}_3\text{N}@C_{80}$ we will show that each of the Sc ions has an effective $3d$ electron count of 0.6. These $3d$ electrons, together with an additional ~ 0.3 electron per Sc transferred to the nitrogen atom are responsible for the strong Sc-N bonding, leaving a total of $(3 \times 2.4) - (3 \times 0.3) = 6.3$ electrons that are donated to the low lying unoccupied molecular orbitals of the C_{80} host molecule, thus stabilizing the highly symmetrical icosahedral C_{80} cage isomer. In agreement with this sixfold electron transfer to the fullerene molecule we use photoemission spectroscopy to show that $\text{Sc}_3\text{N}@C_{80}$ has a sizable energy gap in its electronic excitation spectrum, and note that the detailed fine structure visible in the valence band photoemission spectrum offers further support to the hypothesis that the C_{80} cage has I_h symmetry and thus the endohedral as an entity possesses a tight bunching in energy of its molecular

orbitals. Furthermore, upon K intercalation several $K_x(\text{Sc}_3\text{N}@C_{80})$ phases are formed, as can be determined from the K $2p$ photoemission doublet whose binding energy depends strongly on the chemical environment. The various metallofullerene salts are compared to both $K_x(C_{60})$ and $K_x(C_{70})$, regarding both their electronic structure and charge transfer characteristics.

II. EXPERIMENT

The preparation and separation of $\text{Sc}_3\text{N}@C_{80}$ is described elsewhere.¹¹ Thin films of $\text{Sc}_3\text{N}@C_{80}$ were prepared for photoemission by sublimation onto a clean single crystalline Au(110) surface. The samples were then transferred under ultrahigh vacuum (UHV) conditions into a Perkin Elmer spectrometer, where they were studied using monochromatic Al $K\alpha$ radiation (1486.6 eV) with an energy resolution of 350 meV. The UPS was carried out using the He 1α line (21.2 eV) from a helium discharge lamp with an overall energy resolution of 150 meV. X-ray absorption at the Sc $L_{2,3}$ edge was performed at the VLS-PGM beamline at BESSY; the resolution was 150 meV and the photon energy was calibrated from the binding energy (BE) of Au core level photoemission signals from the clean substrate.

Theoretical simulations of the Sc $L_{2,3}$ XAS spectra were performed using an atomic multiplet approach, which takes the presence of the core hole in the XAS final state explicitly into account. Both the crystal field multiplet (CFM) interactions, as well as the covalency in the form of charge transfer (CT) have been taken into account. The CFM model is a single configuration calculation for Sc ions. The atomic interactions are included for a Sc^{n+} ion and the chemical surroundings are simulated using an electrostatic crystal field. This method has been applied to Sc^{3+} ions with a $3d^0$ configuration in simulations of Sc_2O_3 and ScF_3 .¹⁶ For a $3d^1$ configuration Ti^{3+} ions—which are isoelectronic with Sc^{2+} —have been calculated. The CT model extends the CFM model by using multiple configurations, e.g., $3d^0 + 3d^1\bar{L}$, where \bar{L} stands for an electron transfer from the surroundings (the “ligands,” L) to the central atom.¹⁷ The simplest way to arrive at the effective $3d$ count is by mixing two configurations in the calculations. This approach will be used here.

Intercalation was performed in UHV by evaporating potassium for 10 min from degassed commercial SAES getter sources. During intercalation the sample was held at 450 K. To quantify the degree of intercalation, we used the relative intensity of the K $2p/C\ 1s$ photoemission peaks, taking into account the appropriate photoemission cross section of these states.

III. RESULTS AND DISCUSSION

A. Pristine material

1. The Sc valence state

The Sc_3N unit in $\text{Sc}_3\text{N}@C_{80}$ possesses 12 valence electrons in total. In the context of such an endohedral compound

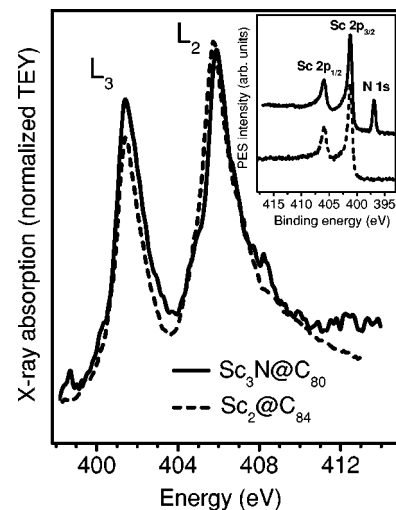


FIG. 1. X-ray absorption spectra of $\text{Sc}_3\text{N}@C_{80}$ and $\text{Sc}_2@C_{84}$ at the Sc $L_{2,3}$ edge. Inset: photoemission spectra of the same materials (solid line: $\text{Sc}_3\text{N}@C_{80}$; dashed line: $\text{Sc}_2@C_{84}$) in the binding energy range covering the Sc $2p$ and N $1s$ core levels.

it is naturally of interest to ask how these charges are distributed between the constituents of the Sc_3N unit and the carbon cage.

Photoemission from the Sc $2p$ levels can give a first rough estimation of the Sc valency from the chemical shift. The observed BE positions in $\text{Sc}_2@C_{84}$ and $\text{Sc}_3\text{N}@C_{80}$ are quite similar (see the inset to Fig. 1), which is the first hint that the Sc ions are close to a formally trivalent Sc (III) state. However, as the net BE of core levels depends not only on the degree of ionization of the atom concerned, but also on the screening of the core hole in the photoemission final state, we have performed XAS measurements at the Sc $L_{2,3}$ edge in order to try and determine the exact degree of charge transfer. As mentioned previously, XAS at the Sc $L_{2,3}$ edge has already been successfully used in this manner⁵ to determine the effective Sc valency in $\text{Sc}_2@C_{84}$ to be 2.6 (i.e., $\text{Sc}\ 3d^{0.4}$).

Figure 1 displays the XAS spectra of both $\text{Sc}_3\text{N}@C_{80}$ and $\text{Sc}_2@C_{84}$. The $\text{Sc}_3\text{N}@C_{80}$ spectrum shows a more intense Sc L_3 peak and new shoulders appear on the high energy sides of both main Sc peaks compared to $\text{Sc}_2@C_{84}$. These subtle differences show that the effective valency in both compounds is not exactly the same. This is related to a different interaction of the encaged cluster with the carbon cage and within the cluster itself. In order to quantify the effective valency, we compare the data with CFM-CT simulations, such as those shown in Fig. 2 for the Sc $L_{2,3}$ edges. The topmost spectrum displays the simulation for ionic Sc^{2+} where the ground state is $[\text{Ar}]3d^1$, the bottommost spectrum the one of ionic Sc^{3+} with the $[\text{Ar}]3d^0$ ground state. The experimental spectrum obviously does not match either of these extreme configurations but rather lies in between. This indicates that hybridization effects have to be taken into account. The best agreement between the simulation and the experimental data is achieved for a 60% admixture of the $3d^1$ configuration (Fig. 2), leading to an effective degree of ionization of close to 2.4 electrons per Sc, i.e., a formal

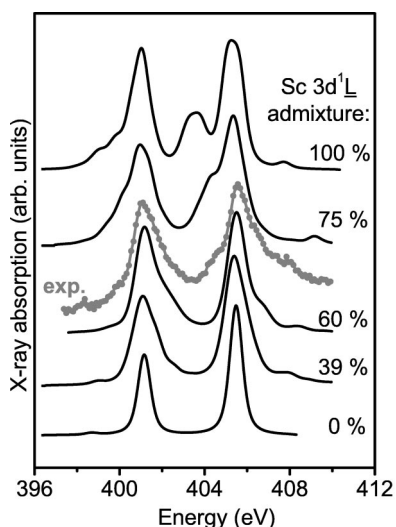


FIG. 2. Thin solid lines: simulations of the Sc $L_{2,3}$ XAS spectrum of $\text{Sc}_3\text{N}@C_{80}$ using a crystal field atomic multiplet model including the effects of charge transfer. The percent values indicate the degree to which a $3d^1\bar{L}$ (\bar{L} stands for ligand hole) configuration was admixed with the $3d^0$ configuration in the ground state. Gray line with symbols: the experimental Sc $L_{2,3}$ XAS spectrum of solid $\text{Sc}_3\text{N}@C_{80}$. The agreement is at its best for a 60% $3d^1$ admixture, corresponding to a Sc $3d$ electron count in the ground state of 0.6.

Sc $3d$ electron count of 0.6 per Sc. This result shows that the valence state of the Sc atoms in $\text{Sc}_3\text{N}@C_{80}$ ($3d^{0.6}$) is reduced as compared to that in $\text{Sc}_2@C_{84}$ ($3d^{0.4}$), which is consistent with the existence of significant intracluster interactions within the Sc_3N unit compared to the loosely bound Sc ions in $\text{Sc}_2@C_{84}$.¹⁸

2. The charge distribution within the encapsulated Sc_3N cluster and charge transfer to the fullerene cage

At this stage it is useful to review what one's expectations could be as regards the charge distribution in this system. Despite it being a grave oversimplification (as shown by the experimentally determined fractional Sc $3d$ electron count), we open by discussing a purely ionic model. If each Sc of the Sc_3N cluster were to transfer one electron to the N, the latter would formally have a closed shell and the remaining six Sc valence electrons could then be transferred to the C_{80} cage leaving the Sc ions in a formally trivalent, $3d^0$ Sc^{3+} state. According to the results of a number of calculations, of the seven isomers of C_{80} satisfying the isolated pentagon rule (IPR), the I_h isomer is predicted to be the *least* stable in the neutral state because of its fourfold degenerate highest occupied molecular orbital (HOMO) which contains only two electrons.^{2,3,7,13–15} This situation is unstable with respect to a Jahn–Teller distortion of the molecule, resulting in a split-off HOMO (two electrons) and an unoccupied, threefold degenerate lowest unoccupied molecular orbital (LUMO). Thus, if the C_{80} molecule was then to receive six additional electrons, the new LUMO could then be completely filled, resulting in a large gap, closed-shell, stable structure.¹⁵ This effect is predicted to make the I_h C_{80} cage the most stable among the

seven IPR isomers not only in the $(C_{80})^{6-}$ charge state^{2,3,7,13–15} but also (to a lesser extent) in a $(C_{80})^{4-}$ charge state.¹³

The problem with the simple picture given in the opening paragraph of this section is that the experimental XAS data offer no support for a simple $3d^0$ Sc^{3+} -like scenario: there is clearly finite $3d$ electron density at the Sc site. The key here is to take the short Sc–N bond length into account (1.98 Å in the endohedral vs 2.25 Å in bulk ScN—Ref. 19). As ScN is quite an ionic compound, the shorter Sc–N distance in the endofullerene is a signal of significant Sc/N covalence. This sharing of electron density will naturally lead to increased charge density at the Sc, thus accounting for the $3d^{0.6}$ configuration of the Sc ions. This hypothesis receives support from the planar (i.e., *not* ammonia-like) form of the Sc_3N cluster, which is consistent with a significant $p_\pi-d_\pi$ (“back-donation”) component in the Sc–N bonding,¹⁸ in which only 0.3 electrons per Sc are fully transferred to N.²⁰ As a result of the observed formal Sc $3d^{0.6}$ configuration in $\text{Sc}_3\text{N}@C_{80}$, and based on the foregoing one can propose that $(3 \times 2.4) - (3 \times 0.3) = 6.3$ electrons are available for transfer from a Sc_3N cluster on its encapsulation in a C_{80} molecule,²¹ thus providing the six electrons required to optimally stabilize the I_h C_{80} cage as discussed previously.

In an alternative view of the Sc–N bonding one electron per Sc would be considered to be fully transferred to N (and 0.6 $3d$ electrons per Sc remain on the transition metal). Then $(3 \times 2.4) - 3 = 4.2$ electrons are available for transfer to the C cage. Considering the short Sc–N distance in this system, however, it is likely that in this way the N electron density is underestimated, as some of the Sc $3d^{0.6}$ electron density is certainly participating in the $p_\pi-d_\pi$ covalent bonding. Consequently, the N would then have, in fact, more than the eight electrons it requires in its outer shell. However, pursuing this avenue further for the sake of argument, one could thereby arrive at a net stabilization of the I_h C_{80} isomer in its four minus charge state,¹³ which would be needed to explain the ^{13}C NMR data.¹⁰ Incidentally, a four minus charge on the host cage would also be one way to explain the different retention time of $\text{Sc}_3\text{N}@C_{80}$ in chromatographic separation compared to systems such as $\text{La}_2@C_{80}$, which are taken to be close to the ionic limit of sixfold electron transfer¹⁰ (although the results of Refs. 22 and 1 warn us that an ionic picture even for $\text{La}@C_{82}$ is an oversimplification). Nevertheless, both the issues regarding the undercounting of the effective electron density accessible to the nitrogen given previously and the large binding energy of the highest occupied electronic states of solid $\text{Sc}_3\text{N}@C_{80}$ observed in the valence band photoemission data presented in the following are strong arguments against this “four minus” picture and in favor of a $(C_{80})^{6-}$ scenario.

3. Valence band photoemission

In valence band photoemission spectroscopy the matrix-element weighted occupied density of states is probed, and one can thereby gain information not only regarding the energy distribution of the electronic states but also about the symmetry and the stability of the metallofullerene in ques-

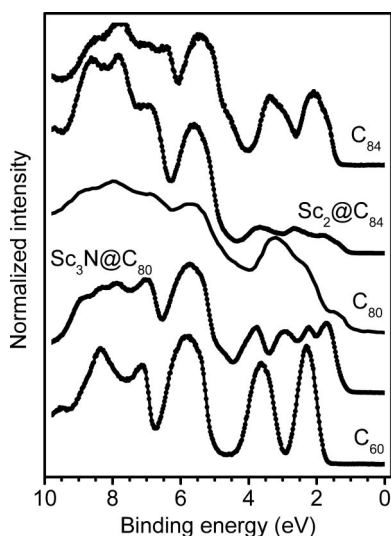


FIG. 3. Valence band photoemission spectra of the metallofullerenes $\text{Sc}_3\text{N}@C_{80}$ and $\text{Sc}_2@C_{84}$, with the analogous spectra of the “empty” fullerenes C_{60} , C_{80} , and C_{84} shown for comparison. The spectrum of C_{80} is taken from Ref. 12.

tion. The He I photoemission spectra shown in Fig. 3 are mainly due to emission from the carbon cage states, a conclusion drawn from photoionization cross-section considerations. For $\text{Sc}_3\text{N}@C_{80}$ the ratio between atomic photoionization cross sections for C $2p$, Sc $3d$, and N $2p$ emission leads to an upper limit for the contribution from the Sc_3N unit to the overall photoemission response upon using He I radiation of only about 2%. Generally, the valence bands of higher fullerenes and metallofullerenes display broad structures in photoemission, this breadth reflecting the splitting of electronic states due to the (generally) low symmetry of the carbon cage and due to covalent interactions between the engaged metal and the host molecule. As typical examples, the spectra of $\text{Sc}_2@C_{84}$ and C_{84} are also depicted in Fig. 3. In contrast, $\text{Sc}_3\text{N}@C_{80}$ exhibits four narrow peaks in the low energy region ($\text{BE} < 5$ eV) of its valence band photoemission spectrum. This would be fully consistent with the suggestion that the carbon cage possesses high, icosahedral symmetry. Indeed, the spectrum of $\text{Sc}_3\text{N}@C_{80}$ is more comparable to that of C_{60} (I_h) than to that of pristine C_{80} . In conclusion, compared to pristine C_{80} which has low, D_2 symmetry,¹² we observe well-defined, sharp photoemission features for $\text{Sc}_3\text{N}@C_{80}$ pointing to the high degeneracy of the electronic states, concomitant with I_h symmetry of the fullerene cage. The fact that the $\text{Sc}_3\text{N}@C_{80}$ molecule as a whole has only C_3 symmetry (or even is reduced to C_1 in the solid state¹⁸) evidently does not give rise to a lifting of the degeneracy of C_{80} 's molecular orbitals visible above the vibronic broadening which dominates the width of the individual molecular orbitals in valence band photoemission. Thus, in the $\text{Sc}_3\text{N}@C_{80}$ molecule, the majority of the electronic levels remain quite tightly bunched in energy.

A further point of interest in the valence band spectrum of $\text{Sc}_3\text{N}@C_{80}$ is the fact that the onset of the HOMO is at the relatively large binding energy of ~ 1 eV. The well-known electron correlation effects in the fullerenes^{23,24} mean that in

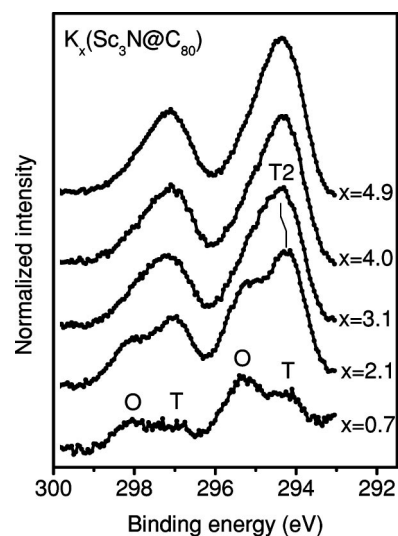


FIG. 4. $K 2p$ core level photoemission spectra for the system $\text{K}_x(\text{Sc}_3\text{N}@C_{80})$ as a function of increasing K intercalation level, x . The labels T and O refer to signal originating from K ions situated in interstitial sites of a tetrahedral or octahedral type, respectively.

an ionizing spectroscopy such as photoemission this onset energy cannot necessarily be interpreted simply as an expression of the minimal energetic separation of the HOMO and LUMO. Nevertheless, the BE of this onset is too large to be consistent with an odd-electron system, such as is approximated in certain endohedrals such as $\text{M}@C_{82}$ [$\text{M} = \text{Gd}, \text{La}$]. The onset energy is also such that it presents a strong argument in favor of a $(C_{80})^{6-}$ scenario in $\text{Sc}_3\text{N}@C_{80}$, as the further Jahn–Teller splitting of a threefold degenerate LUMO (such as that of the C_{80} molecule) containing four electrons would not be able to account for the magnitude of the observed gap in the electronic excitation spectrum, whereas a sixfold electron transfer to the I_h C_{80} cage would result in a closed-shell structure with the excitation gap then corresponding to a large extent to the (large) LUMO – LUMO+1 energy separation. We note that the theoretical predictions of an energy gap of about 2 eV for both $(C_{80})^{6-}$ and $\text{Sc}_3\text{N}@C_{80}$ are in qualitative agreement with our observation.^{15,18}

B. K-doped material

This part of the paper deals with additional (so-called “combinational”) doping of the metallofullerene $\text{Sc}_3\text{N}@C_{80}$ by K intercalation. From x-ray photoemission (XPS) measurements, the intensity ratio between the $K 2p$ and $C 1s$ lines can give a good indication of the overall potassium concentration in such intercalation compounds. Figure 4 displays the $K 2p$ photoemission lines for several intercalation levels in $\text{K}_x(\text{Sc}_3\text{N}@C_{80})$. Similar to pristine fullerenes, many metallofullerenes crystallize at room temperature in a fcc-like close-packed structure.²⁵ Hence, both octahedral and tetrahedral interstitial sites can serve as hosts for the K ions (respectively, labeled O and T in Fig. 4) and this leads to different $K 2p$ peak positions in the photoemission spectra due to their different Madelung potentials.^{26,27} In previous

data from K intercalated fullerenes, the features evolving upon intercalation have been related to the phase diagrams of K_xC_{60} and K_xC_{70} .^{27–29} Thus, in analogy with the situation in these systems, the observation of two $K 2p$ doublets—indicating the occupation of two different interstitial lattice sites—right from the outset of intercalation, is consistent with an fcc-like structure for $Sc_3N@C_{80}$. The doublets corresponding to the octahedral and tetrahedral sites are observed at 298 and 295.3 eV, and at 296.9 and 294.1 eV, respectively (with the energy separation of each component of the same doublet equal to the well known spin–orbit splitting of the $K 3p_{1/2}$ and $K 3p_{3/2}$ levels). For an average stoichiometry $K_{0.7}(Sc_3N@C_{80})$, both tetrahedral and octahedral sites are occupied but the latter site is favored (see the bottommost spectrum of Fig. 4). In K_xC_{60} for $x < 3$, at room temperature, phase separation between C_{60} and K_3C_{60} is observed,^{27,28} giving rise to a constant O to T intensity ratio of 1:2, independent of the average potassium stoichiometry. Only above 450 K is a stable phase K_1C_{60} observed, in which only the octahedral site is occupied. A similar kind of phase separation is observed for K_xC_{70} but between the C_{70} and K_1C_{70} phases.²⁹ At room temperature, stable K_xC_{70} phases are observed for $x = 1, 4$ and 6 .²⁹ In the light of this behavior in the system K_xC_{70} , the predominant occupancy of octahedral site in $K_{0.7}(Sc_3N@C_{80})$, signaled by the more intense O component in Fig. 4, is probably correlated to the formation of a $K_1(Sc_3N@C_{80})$ phase.

Upon further intercalation, the O site feature reduces in intensity with respect to the T peak, consistent with the formation of a fcc-like $K_3(Sc_3N@C_{80})$ phase. This behavior is in contrast to doped C_{70} where a switch from a fcc- to a bcc-like lattice is observed for $x > 1$. In our case, only for higher doping $x > 3$, does such a transformation into a body centered structure appear to occur. This is similar to the K_xC_{60} case and is confirmed by the observation of a new $K 2p$ doublet (marked as T_2 at 297.2 and 294.3 eV in Fig. 4), related to a body centered crystal symmetry. This is consistent with the formation of a stable phase $K_4(Sc_3N@C_{80})$ or $K_6(Sc_3N@C_{80})$ as in K_xC_{60} . This observed doping dependence is also typical of other metallofullerenes, as can be seen by the example of potassium intercalated $Tm@C_{82}$.³⁰

Additional information can be extracted from the $C 1s$ core level of the C_{80} cage and the $N 1s$ and $Sc 2p$ core level spectra of the nitride unit. We deal first with the $C 1s$ spectrum of the pristine endohedral before going into the doping dependence. C_{60} , with its icosahedral molecular symmetry, possesses only a single C site, giving rise to a $C 1s$ core level photoemission line shape which is symmetric with a full width at half maximum (FWHM) of 0.65 eV. In the preceding, strong arguments have been presented—over and above the ^{13}C NMR data¹⁰—for the icosahedral molecular symmetry of the C_{80} cage in $Sc_3N@C_{80}$. Empty $I_h C_{80}$ possess two inequivalent C sites, whereas the endohedral molecule has lower overall symmetry due to the presence of the encapsulated Sc_3N unit. The latter has indeed been suggested to interact in a bonding sense via the Sc atoms with the corannulene units of the carbon cage, but nevertheless does not lead to a significant distortion of the C_{80} cage itself.¹⁸ This

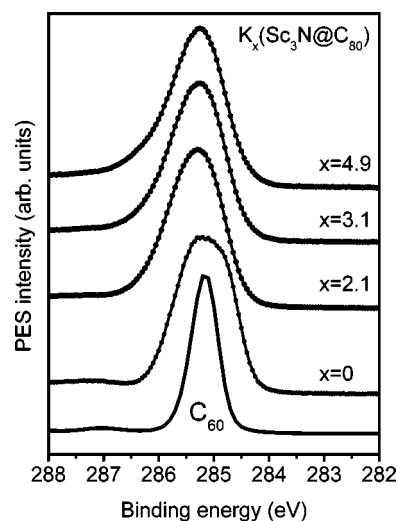


FIG. 5. X-ray photoemission spectra of $K_x(Sc_3N@C_{80})$ at the $C 1s$ core level as a function of increasing K intercalation. The $C 1s$ spectrum of C_{60} (gray) is shown for comparison.

cluster–cage interaction could well be the source of the larger FWHM of the $C 1s$ core level line of 1.2 eV for the C_{80} endohedral, compared to the FWHM of 0.7 eV recorded for C_{70} ,²⁴ an empty fullerene also possessing two inequivalent C sites. However, the results of the valence band photoemission, taken together with the absence of a strong distortion of the C_{80} host cage¹⁸ suggests that the cluster–fullerene interaction does not lead to a large energetic splitting between the molecular orbital-derived electronic states which would be formally degenerate in a hypothetical $I_h Sc_3N@C_{80}$ molecule.

Returning to the question of the doping dependence of the core level spectra, we note that the $C 1s$ peak evolution in $Sc_3N@C_{80}$ upon intercalation, displayed in Fig. 5, is completely different compared to the situation found in C_{60} and C_{70} , with the $C 1s$ peak sharpening upon intercalation (the width being reduced by about 8% on going from $x = 0$ to $x = 3.1$). Therefore, in contrast to the C_{60} intercalation compounds, doping possibly leads to a higher degree of equivalence for the carbon sites of the C_{80} cage. We also note that the peak remains nearly symmetric at every stage of intercalation, like in the case of $K-C_{70}$ ²⁹ and unlike $K-C_{60}$ ²⁸ and other metallofullerenes.³⁰ Furthermore, unlike both intercalated C_{60} and C_{70} , the peak position shifts toward higher binding energy for $x = 2.1$ (from 285.2 to 285.3 eV) and then goes back to 285.25 eV for $x = 3.1$. The origin of such a nonrigid shift could be related to the pinning of the Fermi level in the different $K_x(Sc_3N@C_{80})$ phases. In addition, the individual separation between the newly occupied HOMO levels and the Fermi level is strongly altered by the local C_{80} cage structure, with the consequence that the shift of the $C 1s$ line cannot be explained within a simple rigid band model. A more accurate analysis is required with the aid of sample distillation, for instance, in order to get more precise information on the phases that are present in the crystal. Until this is carried out, the behavior of the $C 1s$ BE upon doping remains an open question.

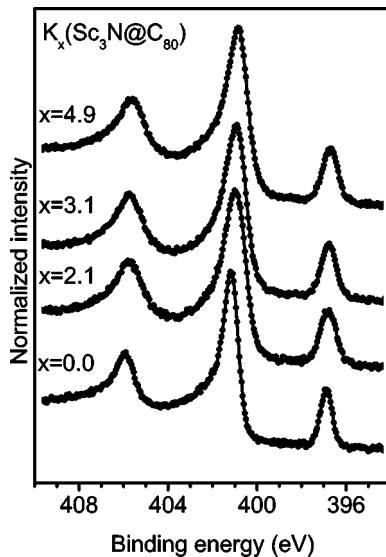


FIG. 6. Core level photoemission spectra of the Sc $2p$ and N $1s$ lines at several stages of K intercalation in $K_x(\text{Sc}_3\text{N}@C_{80})$.

We now discuss the changes of the core level data from the engaged cluster upon intercalation. Figure 6 shows the Sc $2p$ and N $1s$ peaks as a function of K content. It is obvious from the data that these electronic states are scarcely altered by the doping process. For increasing potassium concentration, a small broadening of the core level spectra of about 250 meV is observed. This broadening can be explained by screening effects due to the polarizable potassium counterions: similar effects have been seen in Tm $4d$ and Tm $4f$ photoemission from $K_x\text{Tm}@C_{82}$.³⁰ For the Sc $3d$ absorption edge in XAS, no changes of the line shape and of the peak intensities are observed upon intercalation. This makes it clear that the effective Sc valency is not altered with intercalation-induced doping of the metallofullerene. This is in good agreement with recent doping experiments on other metallofullerenes such as $\text{Sc}_2@C_{84}$, $\text{Tm}@C_{82}$, $\text{Gd}@C_{82}$, $\text{Ce}_2@C_{74}$.³⁰

The valence band photoemission spectra at various K intercalation levels are presented in Fig. 7. At very low doping, the Fermi level can be assumed to be pinned near the edge of the lowest unoccupied molecular orbital (LUMO),³¹ thus making the onset observed at 1.1 eV a more accurate estimation of the band gap relevant for ionization of the molecule (second spectrum from the bottom). From $x=0.7$ and upwards, filling of the LUMO gives rise to a broad structure at about 1.5 eV binding energy. Subsequent doping leads to the appearance of several $K_x(\text{Sc}_3\text{N}@C_{80})$ phases, with the superposition of their different photoemission signatures giving rise to broad spectral structures. Thus the very sharp peaks observed near the Fermi level in the pristine material merge into structureless features in the valence band of the intercalated material.

IV. CONCLUSIONS

We have presented a systematic study of the electronic structure and charge transfer characteristics of the novel

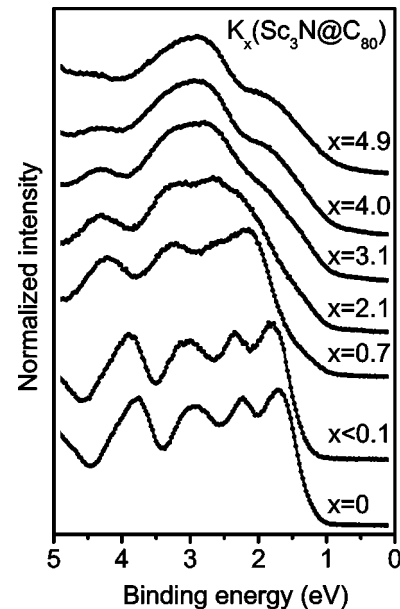


FIG. 7. Valence band photoemission spectra of $K_x(\text{Sc}_3\text{N}@C_{80})$ at several stages of K intercalation.

trinitride endohedral fullerene $\text{Sc}_3\text{N}@C_{80}$ in the solid state, both in its pristine and K intercalated forms.

As regards the pristine endofullerene, existing spectroscopic and theoretical results,¹⁸ taken together with the Sc $L_{2,3}$ XAS (experiment and cluster-based simulation) and photoemission data presented here show the following:

- (1) the effective $3d$ electron count at the Sc sites is 0.6 electrons (compared to a Sc $3d^{0.4}$ configuration in $\text{Sc}_2@C_{84}$),
- (2) there is strong covalent bonding between the Sc and the N in the encapsulated cluster,
- (3) the onset in photoemission of the highest occupied molecular orbitals is ~ 1 eV below E_F ,
- (4) the valence band photoemission spectrum of solid $\text{Sc}_3\text{N}@C_{80}$ shows a wealth of fine structure, more reminiscent of that of C_{60} than of a typical higher-fullerene endohedral,
- (5) the C $1s$ core level spectrum of $\text{Sc}_3\text{N}@C_{80}$ shows a relatively narrow main line for an endohedral fullerene, whose fine-structure suggests the presence of only two inequivalent C sites.

These facts can be consistently explained in a picture in which a significant degree of $d_{\pi}-p_{\pi}$ covalent “backbonding” within the Sc_3N unit is responsible for the finite $3d$ electron density at the Sc site, with the remaining valence electron density from the Sc_3N cluster being transferred to fully populate the lowest lying C $2p$ -derived π^* molecular orbital. This leads, in terms of C_{80} 's LUMO population with respect to the neutral molecule, to a hexaanionic state for the fullerene cage. This $(C_{80})^{6-}$ state is the clue to understanding the photoemission data, as both the narrow C $1s$ line as well as the large gap in the valence band photoelectron spectrum are to be expected only for the case in which the struc-

ture of the C_{80} host cage has high, I_h symmetry and a fully closed shell. This C_{80} isomer is highly unstable in its neutral form, but is predicted to be the most stable isomer in a hexaanionic state. Thus, the data presented here, together with the solution ^{13}C NMR results¹⁰ serve to put the I_h identity of the C_{80} carbon cage in this endohedral beyond doubt.

In addition, by analyzing the evolution of the $K 2p$ core level photoemission features as a function of intercalation, and comparison of the results with the K intercalated C_{60} and C_{70} systems, we were able to give evidence compatible

with the formation of several distinct phases in the $K_x(\text{Sc}_3\text{N}@C_{80})$ system.

ACKNOWLEDGMENTS

This work was supported by the EU-sponsored TMR Research Network ‘‘FULPROP’’ (ERBFMRXCRT-970155). In addition, T.S. thanks the BMBF (05 5F8BD11) and T.P. the ÖAW and FWF for funding. Our thanks also to Gotthardt Seifert for useful discussions.

- ¹B. Kessler, A. Bringer, S. Cramm, C. Schlebusch, W. Eberhardt, S. Suzuki, Y. Achiba, F. Esch, M. Barnaba, and D. Cocco, *Phys. Rev. Lett.* **79**, 2289 (1997).
- ²K. Kobayashi *et al.*, *Chem. Phys. Lett.* **245**, 230 (1995).
- ³K. Kobayashi and S. Nagase, *Chem. Phys. Lett.* **262**, 227 (1996).
- ⁴T. Pichler, M. S. Golden, M. Knupfer, J. Fink, U. Kirbach, P. Kuran, and L. Dunsch, *Phys. Rev. Lett.* **79**, 3026 (1997).
- ⁵T. Pichler, Z. Hu, C. Grazioli, S. Legner, M. S. Golden, M. Knupfer, J. Fink, F. M. F. de Groot, M. R. C. Hunt, P. Rudolf, R. Follath, C. Jung, L. Kjeldgaard, P. Brühwiler, M. Inakuma, and H. Shinohara, *Phys. Rev. B* **62**, 13 196 (2000).
- ⁶T. Schwieger, H. Peisert, M. Knupfer, M. S. Golden, J. Fink, T. Pichler, H. Kato, and H. Shinohara, *International Workshop on the Electronic Properties of Novel Materials*, Kirchberg, Austria, 2000 [AIP Conf. Proc. **544**, 142 (2000)].
- ⁷T. Takahashi, A. Ito, M. Inakuma, and H. Shinohara, *Phys. Rev. B* **52**, 13 812 (1995).
- ⁸B. W. Smith, M. Monthieux, and D. E. Luzzi, *Nature (London)* **396**, 323 (1998).
- ⁹B. W. Smith, D. E. Luzzi, and Y. Achiba, *Chem. Phys. Lett.* **331**, 137 (2000).
- ¹⁰S. Stevenson, G. Rice, T. Glass, K. Harich, F. Cromer, M. R. Jordan, J. Craft, E. Hadju, R. Bible, M. M. Olmstead, K. Maltra, A. J. Fisher, A. L. Balch, and H. C. Dorn, *Nature (London)* **401**, 55 (1999).
- ¹¹L. Dunsch, A. Bartl, P. Georgi, and P. Kuran, *Synth. Met.* **121**, 1113 (2001).
- ¹²T. R. Cummins, M. Bürk, M. Schimdt, J. F. Armbruster, D. Fuchs, P. Adelman, S. Schuppler, R. H. Michel, and M. M. Kappes, *Chem. Phys. Lett.* **261**, 228 (1996).
- ¹³P. W. Fowler and F. Zerbetto, *Chem. Phys. Lett.* **243**, 36 (1995).
- ¹⁴D. E. Manomopoulos and P. W. Fowler, *Chem. Phys. Lett.* **187**, 1 (1991).
- ¹⁵K. Nakao, N. Kurita, and M. Fujita, *Phys. Rev. B* **49**, 11 415 (1994).
- ¹⁶F. M. F. de Groot, J. C. Fuggle, B. T. Thole, and G. A. Sawatzky, *Phys. Rev. B* **41**, 928 (1990).
- ¹⁷F. M. F. de Groot, J. C. Fuggle, B. T. Thole, and G. A. Sawatzky, *Phys. Rev. B* **42**, 5459 (1990).
- ¹⁸M. Krause, H. Kuzmany, P. Georgi, L. Dunsch, K. Vietze, and G. Seifert, *J. Chem. Phys.* **115**, 6596 (2001).
- ¹⁹N. E. Brese and M. O’Keeffe, *Complexes, Clusters and Crystal Chemistry* (Springer, Berlin, 1992).
- ²⁰The N $1s$ binding energy of $\text{Sc}_3\text{N}@C_{80}$ measured in core level photoemission is found at 396.9 eV (see the inset to Fig. 1). Although this is only 300 meV less than in the significantly more ionic AlN [e.g., T. Reier, S. Simson, and J. Schultze, *Electrochim. Acta* **43**, 149 (1998)], as core level binding energies are determined by both chemical shift and Madelung potentials, and are influenced by final state screening effects, a direct comparison of the N $1s$ binding energy does not allow an unambiguous determination of the formal charge on N.
- ²¹Here we mention that the Mulliken charge analysis of $\text{Sc}_3\text{N}@C_{80}$ carried out in Ref. 18 arrives at a Sc d -electron count of 1.4, somewhat higher than that of 0.6 determined from the XAS data. The gross electron populations given in Ref. 18 are built up of a net term describing the unambiguously identifiable electron density within a particular (atomic orbital) basis function and a remaining term coming from the ‘‘sharing out’’ of electron density located in bonds. In the Mulliken approach the latter split is carried out purely on a 50:50 basis, irrespective of the identity of the atoms involved, which can easily lead to an overestimation of the electron population of one of the bonding partners (in this case Sc).
- ²²D. M. Poirier *et al.*, *Phys. Rev. B* **49**, 17 403 (1994).
- ²³R. W. Lof, M. A. van Veenendaal, B. Koopmans, H. T. Jonkman, and G. A. Sawatzky, *Phys. Rev. Lett.* **68**, 3924 (1992).
- ²⁴M. Knupfer, D. M. Poirier, and J. H. Weaver, *Phys. Rev. B* **49**, 2281 (1994).
- ²⁵Y. Li, J. Patrin, M. Chander, J. H. Weaver, K. Kikuchi, and Y. Achiba, *Phys. Rev. B* **47**, 10 867 (1993).
- ²⁶D. M. Poirier, T. R. Ohno, G. H. Kroll, P. J. Benning, F. Stepniak, J. H. Weaver, L. Chibante, and R. E. Smalley, *Phys. Rev. B* **47**, 9870 (1993).
- ²⁷D. M. Poirier, T. R. Ohno, G. H. Kroll, Y. Chen, P. J. Benning, J. H. Weaver, L. Chibante, and R. E. Smalley, *Science* **253**, 646 (1991).
- ²⁸D. M. Poirier and J. Weaver, *Phys. Rev. B* **47**, 10 959 (1993).
- ²⁹M. Knupfer, D. M. Poirier, and J. H. Weaver, *Phys. Rev. B* **49**, 8464 (1994).
- ³⁰T. Pichler, J. Winter, C. Grazioli, M. S. Golden, M. Knupfer, P. Kuran, L. Dunsch, and J. Fink, *Synth. Met.* **103**, 2470 (1999).
- ³¹P. J. Benning, D. M. Poirier, T. R. Ohno, Y. Chen, M. B. Jost, F. Stepniak, G. H. Kroll, J. H. Weaver, J. Fure, and R. E. Smalley, *Phys. Rev. B* **45**, 6899 (1993).